Article:
Farmer, D.A., Brindley, A.A., Hitchcock, A. et al. (6 more authors) (2019) The ChlD subunit links the motor and porphyrin binding subunits of magnesium chelatase. Biochemical Journal, 476 (13). pp. 1875-1887. ISSN 0264-6021

https://doi.org/10.1042/bcj20190095

The ChlD subunit links the motor and porphryin binding subunits of magnesium chelatase

David A Farmer[1], Amanda A Brindley[1], Andrew Hitchcock[1], Philip J Jackson[1,2], Bethany Johnson[1], Mark J Dickman[2], C Neil Hunter[1], James D Reid[3] & Nathan B P Adams[1]

[1] Department of Molecular Biology and Biotechnology, The University of Sheffield, S10 2TN, United Kingdom,

[2] ChELSI Institute, Department of Chemical and Biological Engineering, University of Sheffield, Sheffield S1 3JD, United Kingdom,

[3] Department of Chemistry, The University of Sheffield, S3 7HF, United Kingdom.

Page heading: The ChlD-ChlH interaction in magnesium chelatase

To whom correspondence should be addressed: Dr Nathan B P Adams, Department of Molecular Biology and Biotechnology, University of Sheffield, Firth Court, Western Bank, Sheffield S10 2TN, UK., +44 114 22 22790 nathan.adams@sheffield.ac.uk.

Key Words: magnesium chelatase, ATPase, ATPases associated with diverse cellular activities (AAA), enzyme catalysis, protein-protein interaction, porphyrin, thermophoresis, cross-linking

Abstract

Magnesium chelatase initiates chlorophyll biosynthesis, catalysing the $MgATP^{2-}$ dependent insertion of a Mg^{2+} ion into protoporphyin IX. The catalytic core of this large enzyme complex consists of three subunits: Bch/ChlI, Bch/ChlD and Bch/ChlH (in bacteriochlorophyll and chlorophyll producing species respectively). The D and I subunits are members of the AAA^+ (ATPases associated with various cellular activities) superfamily of enzymes, and they form a complex that binds to H, the site of metal ion insertion. In order to investigate the physical coupling between ChlID and ChlH *in vivo* and *in vitro*, ChlD was FLAG-tagged in the cyanobacterium *Synechocystis* sp. PCC 6803 and co-immunoprecipitation experiments showed interactions with both ChlI and ChlH. Co-production of recombinant ChlD and ChlH in *Escherichia coli* yielded a ChlDH. Quantitative analysis using microscale thermophoresis (MST) showed magnesium-dependent binding (K_d 331 ± 58 nM) between ChlD and H. The physical basis for a ChlD-H interaction was investigated using chemical crosslinking coupled with mass spectrometry (XL-MS), together with modifications that either truncate ChlD or modify single residues. We found that the C-terminal integrin I domain of ChlD governs association with ChlH, the Mg^{2+} dependence of which also mediates the cooperative response of the *Synechocystis* chelatase to magnesium. Our work, showing the interaction site between the AAA^+ motor and the chelatase domain of magnesium chelatase, will be essential for understanding how free energy from the hydrolysis of ATP on the AAA^+ ChlI subunit is transmitted via the bridging subunit ChlD to the active site on ChlH.

Abbreviations

AAA^+, ATPases Associated with various cellular activities; K_d, dissociation constant; D_{IX}, deuteroporphyrin IX; DSF, Differential Scanning Fluorimetry; XL-MS, crosslinking mass spectrometry; MST, microscale thermophoresis; MIDAS, metal ion dependent adhesion site; MgCH, magnesium chelatase; VWFA, von Willebrand factor A; β-DDM, dodecyl-β-maltoside.

Introduction

The first committed step in the biosynthesis of chlorophyll is catalyzed by magnesium chelatase (MgCH; E.C.6.6.1.1), a large, multisubunit enzyme which catalyzes the insertion of a Mg^{2+} ion into protoporphyrin IX in a Mg^{2+} and $MgATP^{2-}$ dependent manner. In photosynthetic organisms MgCH, along with ferrochelatase, lies at the branch point of the chlorophyll and heme biosynthesis pathways. While ferrochelatase is a relatively simple, single subunit enzyme, MgCH is a large complex, with a minimal catalytic requirement of three subunits: in oxygenic phototrophs these subunits are named ChlI, ChlD and ChlH [1–3]. The insertion of a Mg^{2+} ion into protoporphyrin is energetically unfavorable [4,5], and proceeds only *via* coupling to an ATPase motor subunit, ChlI. The ChlI and ChlD subunits are members of the AAA^+ (ATPases associated with various cellular activities) superfamily of enzymes [6]. While ATPase activity has been observed and measured for the ChlI subunit [7–10], no ATPase activity has been observed for ChlD. ChlI hydrolyses $MgATP^{2-}$ to provide the considerable power required to drive Mg^{2+} insertion [5,11]. ChlD appears to act as an allosteric regulator in response to $MgATP^{2-}$ concentrations [12], and the C-terminal domain of ChlD regulates the cooperative response to Mg^{2+} concentrations in the *Synechocystis* sp. PCC 6803 (hereafter *Synechocystis*) MgCH, although not in the *Thermosynechococcus elongatus* enzyme [13]. Previous work has shown the importance of a fully intact ChlD (or bacterial homolog, BchD) protein for maintening chelatase activity [11,13,14], although recent work published by Luo *et al.* [15] suggests only the N-terminal AAA^+ and poly-proline linker domains are required for activity.

The ChlH subunit is a large protein (*ca.* 150 kDa) that binds protoporphyrin IX [16,17]; recent crystallographic evidence has provided clues to the porphyrin binding site [18]. Mg^{2+} and $MgATP^{2-}$ are required for the association of ChlI and ChlD [12,19], mediated by the AAA^+ N-terminal domains of each subunit, whichshare *ca.* 40 % sequence identity. Additionally, ChlD has an extended linker region rich in acidic residues and a C-terminal integrin I domain, which is also known as von Willebrand factor A (VWFA), and these domains are usually associated with protein interactions involving cell adhesion [20]. It is generally assumed that ChlI-D associates with ChlH to form an active ChlIDH complex, but the number and spatial arrangment of subunits required to catalyse the chelatase reaction is currently unknown.

While there have been extensive steady state [2,4,5,12,13,21–26] and transient [27] kinetic analyses of MgCH, there is no settled view on the organisation of subunits and the protein-protein interactions representing the minimal catalytic unit. In addition, it is not known how energy from ATP hydrolysis is transmitted to the catalytic site on ChlH. Here we show that ChlD and ChlH form a complex both *in vivo* and *in vitro*. Using chemical crosslinking coupled with analysis by mass spectrometry (XL-MS) and further biophysical analysis we propose the C-terminal integrin I domain of ChlD forms the majority of interactions with ChlH, with some interaction mediated by the AAA^+ domain of ChlD. This knowledge provides the basis for the organisation of the ChlHID magnesium chelatase complex and for exploring how chemomechanical coupling, produced from the hydrolysis of ATP on the AAA^+ ChlI subunit, is moved to the metal ion insertion site on ChlH via the bridging subunit ChlD.

Materials and Methods

Growth of *Synechocystis*

Strains used in this study are detailed in Table S1. *Synechocystis* strains were grown at 30 °C in BG11 medium [28] buffered with 10 mM N-Tris(hydroxymethyl)methyl-2-aminoethanesulfonic acid (TES)-KOH pH 8.2 (BG11-TES). Starter cultures were grown in a rotary shaker (150 rpm) at a constant illumination of 40 μmol photons m^{-2} s^{-1}. For purification of FLAG-tagged proteins 8 litre cultures of *Synechocystis* were grown with vigorous bubbling with sterile air at a constant illumination of 150 μmol photons m^{-2} s^{-1}. Growth was monitored as the optical density at 750 nm (OD_{750}). For growth on solid medium BG11-TES was supplemented with 1.5 % (w/v) agar, 0.3 % (w/v) sodium thiosulphate and appropriate antibiotics and plates were incubated at 30 °C with 40 μmol photons m^{-2} s^{-1} constant illumination.

Construction of *Synechocystis* strains

Details of primers used in this study are provided in Table S2. To generate strain FLAG-ChlD, the *chlD* gene (slr1777) was amplified from *Synechocystis* DNA with flanking *Not*I and *Bgl*II sites using Q5 High Fidelity DNA polymerase (NEB, UK) and primer pair AH282/AH283. This fragment was cloned into the *Not*I and *Bgl*II sites of pPD-NFLAG [29] such that it was in frame with an N-terminal 3xFLAG tag. The resulting plasmid was

introduced into wild-type *Synechocystis* by natural transformation. Transformants were selected on BG11 agar containing 7.5 μg ml^{-1} kanamycin and genome copies were segregated by sequential doubling of the antibiotic concentration to 60 μg ml^{-1}. Segregation at the *psbAII* locus was confirmed by PCR using primers AH47/AH48 (Fig. S1 A) and the sequence of the FLAG-ChlD encoding gene was verified following amplification from transformant genomic DNA (GATC Biotech, Germany).

To delete the native *chlD* (slr1777) from strain FLAG-ChlDa linear DNA construct was generated to replace 1943 bp of the 2031 bp gene with the zeocin resistance cassette (zeoR). Approximately 500 bp fragments flanking the *chlD* gene were generated by PCR using *Synechocystis* genomic DNA as template with primers AH434/AH435 and AH436/AH437 and zeoR was amplified from pZEO using primers Zeo-F and Zeo-R [30]. These three fragments were purified and used in an overlap extension (OLE)-PCR with primers AH434/AH437, resulting in a *ca*. 2.0 kb product, which was introduced into the FLAG-ChlD strain as above. Transformants were selected on BG11 agar containing 2.5 μg ml^{-1} zeocin and genome copies were segregated by sequential doubling of the antibiotic concentration to 20 μg ml^{-1}. That the native *chlD* was absent in the resulting FLAG-ChlD Δ*chlD* strain was confirmed by PCR with primers AH434/AH437 and AH434/AH438 (Fig. S1 B-C).

Co-production of StrepII-ChlH and ChlD in *E. coli*

The region between the start codon and the end of the hexaHis-tag in pET14bSynChlH [26] was replaced by the region between the start codon and the end of the StrepII-tag (WSHPQFEK) in pET52b (Novagen) by replacing the 92 bp between the *Xba*I and *Nde*I restriction sites with a 95 bp synthetic fragment (Integrated DNA Technologies), generating plasmid pET14bStrepII-SynChlH. The QuikChange II kit (Agilent) was used to introduce an *Spe*I site downstream of the stop codon of *chlH* in pET14bStrepII-SynChlH. The QuikChange II kit was also used to engineer an *Spe*I site downstream of the *Bam*HI site in both pET9aHis-ChlD [12] and pET3a (Novagen), and the *chlD* gene was excised from pET9aHis-ChlD with *Nde*I and *Spe*I and sub-cloned into the same sites of the modified pET3a, producing plasmid pET3aSynChlD. We then used the 'Link and Lock' method [31] to insert *chlD* with its own RBS downstream of the stop codon of the tagged *chlH* gene in pET14bStrepII-SynChlH. The pET3aSynChlD plasmid was digested with *Xba*I and *Hin*dIII and the released fragment was ligated into *Spe*I-*Hind*III cut pET14bStrepII-SynChlH,

creating pET14bStrepII-SynChlH-SynChlD for co-production of N-terminally StrepII-tagged ChlH and untagged ChlD. All plasmids were verified by automated DNA sequencing (GATC, Eurofins Genomics).

Calculation of chlorophyll concentrations in *Synechocystis* strains

Cell number was normalized to OD_{750} and the equivalent of OD_{750} = 1 was mixed directly with a total volume of 1.5 mL methanol and incubated at room temperature for 10 minutes with gentle shaking. Cell debris was cleared via centrifugation at 16000 x *g* for 10 minutes and the concentration of chlorophyll was calculated using the extinction coefficient 71 mM^{-1} cm^{-1} at 665 nm [32].

***In vivo* FLAG-ChlD immunoprecipitations**

Synechocystis strain FLAG-ChlD was grown to an OD_{750} of 0.9. Cells were pelleted and resuspended in buffer A (25 mM sodium phosphate, 50 mM NaCl, 10 mM $MgCl_2$, 10 % (w/v) glycerol pH 7.4 and EDTA-free protease inhibitors). Cells were mixed with an equal volume of 0.1 mm glass beads and broken in a Mini-Beadbeater-16 (BioSpec) (50 seconds beating, 2 minutes cooling on ice, 10 cycles). Soluble proteins and membranes were separated by centrifugation (65000 x *g*, 30 minutes, 4 °C). The membrane fraction was washed with an excess of buffer A, then resuspended in buffer A with 1.5 % (w/v) dodecyl-β-maltoside (β-DDM, Applichem) and solubilised for 2 hours at 4 °C. The solubilized membranes were separated from insoluble material by centrifugation (65000 x *g*, 30 minutes, 4 °C).

FLAG-ChlD and associated proteins were purified from the soluble and membrane fractions using an 200 μL anti-FLAG-M2 agarose columns (Sigma-Aldrich) equilibrated in buffer A (+ 0.25 % (w/v) β-DDM for membrane fraction). FLAG-ChlD was eluted with 500 µL of buffer A (+ 0.25 % β-DDM for membrane fraction) containing 150 µg/mL 3xFLAG peptide (Sigma-Aldrich).

The FLAG-ChlD co-immunoprecipitation complex was seperated by denaturing gel electrophoresis using NuPage 12 % Bis-Tris gels (Life Technologies) and proteins were transferred onto a polyvinylidine fluoride membrane for immunodetection. Immunoblotting and detection were performed as described previously [29].

Purification of Strep-II tagged ChlH

The pET3aStrepII-SynChlH-SynChlD was transformed into *E. coli* Rosetta™(DE3)pLysS, and grown in 2xYT media to an OD_{600} of 0.6 where protein overproduction was induced with the addition of 0.4 mM IPTG and flasks incubated for a further 12 hours at 16 °C. Cells were suspended in binding buffer (100 mM Tris, 1 mM EDTA, pH 8) and lysed by sonication (6 x 30 s with 30 s breaks), and cell debris cleared by centrifugation (15 m, 21 k RPM). The supernatant was applied to a StrepTrap HP column (GE Healthcare) pre-equilibrated in binding buffer, and unbound proteins removed with 15 column volumes of binding buffer. ChlH-StrepII was eluted with binding buffer supplemented with 2.5 mM desthiobiotin. Western blot analysis was performed in essentially the same manner as described above.

The control experiment with nontagged ChlD was grown and purified in an identical fashion.

Purification of chelatase subunits

Production and purification of MgCH subunits was performed as described previously [5,12,13]. Point mutants were produced using the QuikChange II site directed mutagenesis kit (Agilent, UK) with the primers listed in Table S3 and verified by sequencing (GATC Biotech).

Thermophoresis

ChlH or ChlD was labelled with NHS-NT647 dye (NanoTemper Technologies, Munich, Germany) according to the manufacturer's instructions before being exchanged into microscale thermophoresis (MST) buffer (50 mM Tris/NaOH, 0.2 % pluronic F-127, with or without 10 mM MgCl, pH 7.8). MST experiments were performed in triplicate, with 20 nM labelled chelatase subunit titrated with a serial dilution of partner protein. Samples were loaded into premium capillaries (NanoTemper Technologies) and illuminated with 20 % RED LED power, with thermophoresis induced with 40 % IR laser power. Thermophoresis data was analysed as previously described [11].

Chemical cross-linking of proteins

Purified ChlH was desalted into activation buffer (100 mM MES, 0.5 M NaCl, pH 6) using a Zeba Spin column according the manufacturer's instructions. 1 mg ml^{-1} of ChlH in 100 µL activation buffer was incubated with 2 mM 1-ethyl-3-[3-dimethylaminopropyl]carbodiimide hydrochloride (EDC, Thermo Fisher) and 5 mM N-hydroxysuccinimide (NHS, Sigma

Aldrich) at room temperature for 15 minutes and then buffer exchanged into PBS. 1 mg ml^{-1} activated ChlH was mixed with 1 mg ml^{-1} ChlD and incubated at 34 °C for two hours prior to flash-freezing samples.

Cross-linked samples were analysed by SDS-PAGE using NuPAGE 3-8 % Tris-acetate gels in denaturing buffer (Tris-glycine-SDS), and cross-linked protein detected by immunoblotting for *Synechocystis* ChlD and ChlH, using the methods reported above.

In-gel digestion and mass spectrometry analysis

Bands corresponding to putative ChlH-ChlD complexes were excised and subjected to in-gel digestion with trypsin according to [33]. The peptide extracts were dried in a vacuum centrifuge, redissolved in 10 µL 0.1 % (v/v) TFA, 3 % (v/v) acetonitrile and 2 µL analysed by nano-flow liquid chromatography (Ultimate 3000 RSLCnano system, Thermo Scientific) coupled to a mass spectrometer (Q Exactive HF, Thermo Scientific) according to [34]. The mass spectra were processed with Byonic v. 2.9.38 (Protein Metrics, CA, USA) with parameters set to default except that carbamidomethyl-Cys and Met oxidation were specified as fixed and variable (common) modifications respectively. Protein identifications were made by searching the Cyanobase *Synechocystis* sp. PCC 6803 proteomic database (http:// www.uniprot.org/uniprot/?query=organism:1111708) using the Byonic search engine (Protein Metrics). The identification of crosslinked peptides was enabled by manually creating a rule for EDC with the following syntax: 'EDC / -18.010565 @ K,D,E | xlink'. Crosslinked peptides were identified in Byonic using a two-dimensional posterior error probability (2-D PEP) $<$ 0.01 as a threshold. All crosslinked peptides identified in Byonic were manually verified.

Kinetic assays of magnesium chelatase activity and data analysis

Kinetic assays were performed as described previously [12]. Analysis was conducted in MARS Data Analysis Software Version 1.x R2 (BMG Labtech) and Igor Pro Version 7.0.6.1 (Wavementrics, Lake Oswego, OR)

Producing a homology model for the integrin I domain of ChlD

Residues 481-672 of the *Synechocystis* enzyme were highlighted by Prosite [35] to belong to the VWFA family. These residues were aligned using HHPRED [36] against sequences with

known structures in the PDB. An alignment with hit TEM8 was generated using the HHPRED-TemplateSelection tool and this alignment used to create a model with Modeller (v9.21) [37].

Differential scanning fluorimetry (DSF) assays for thermal stability of MIDAS mutants

Each assay contained 5 µM ChlD, 10 mM $MgCl_2$ 1x SYPRO Orange and 1x protein buffer to give a final volume of 50 µL. The QPCR machine (Agilent) was programmed to generate a temperature increase of 1 °C per cycle per minute. A fluorescence reading was taken each cycle. Melting temperatures (T_m) were assigned at the point where 50 % of the protein is unfolded, as determined by fitting melting data to a sigmoid Boltzmann distribution (Eq. 3) where F_0 is initial fluorescence, F_{max} is maximal fluorescence, T is the temperature, T_m is the melting temperature and T_0 is the initial temperature.

$$F = F_0 + \left(\frac{F_{max}}{1+\exp^{\frac{T_M - T_0}{\frac{\delta T}{\delta F}}}} \right) \quad (3)$$

CD spectrometry of MIDAS mutants

Spectra were recorded with a JASCO-810 spectrometer (JASCO, Great Dunmow, UK). Protein (0.05 mg ml^{-1} was in a 5 mM sodium phosphate buffer, 1 mM β-mercaptoethanol, pH 7.5. Spectra were recorded from 260 to 200 nm (1 nm steps, 4 s nm^{-1}, 4 accumulations) and background subtracted.

Results

***Synechocystis* ChlH and ChlD form a membrane-associated complex *in vivo*.**

To investigate the *in vivo* association of ChlD with the other chelatase subunites, we constructed a *Synechocystis* strain producing ChlD with a 3xFLAG-tag encoded at the N terminus expressed under the control of the *psbAII* promoter (FLAG-ChlD), and then deleted the native *chlD* gene from this strain (FLAG-ChlD Δ*chlD*). (Fig. S1, Table S1). The cellular concentrations of chlorophyll in wild-type, FLAG-ChlD and FLAG-ChlD Δ*chlD* were similar (data not shown). Soluble and membrane fractions were prepared from photoautotrophically grown FLAG-ChlD strains, then membranes were solubilized in buffer containing 1.5 % (w/v) β-DDM and the extracts applied to an anti-FLAG column. After extensive washing, eluted material was separated by SDS-PAGE and specific antibodies for

ChlH and ChlD were used to determine the presence of ChlH and ChlD (Fig. 1 A). In both soluble and membrane fractions, ChlH co-purifies with FLAG-ChlD (Fig. 1 A, lanes S and M respectively).

Despite not being integral membrane proteins, both ChlD and ChlH proteins are present in higher concentrations in the membrane fraction than in the soluble fraction (compare lanes S and M, Fig. 1 A). The ChlD protein appears to be unstable both *in vitro* and *in vivo*, and a *ca.* 50 kDa breakdown product is evident when blotting for either ChlD or the FLAG-tag, indicating the 50 kDa fragment is from the N-terminal region of the protein. We further analyzed the membrane fraction, using immunoblots to probe for each obligate subunit of MgCH (ChlI, ChlD and ChlH) in fractions of membranes from WT and FLAG-ChlD Δ*chlD* strains (Fig. 1 B). This analysis revealed that the entire chelatase complex can be purified from the membrane fraction using the FLAG-tagged ChlD protein. No chelatase subunits bound to the anti-FLAG column in the absence of the FLAG tag on ChlD (see WT lanes, Fig. 1 B). We note that when purified *in vitro* MgCH is a soluble protein complex, and does not require detergents for purification or activity, and indeed the addition of detergent decreases the *in vitro* activity of MgCH.

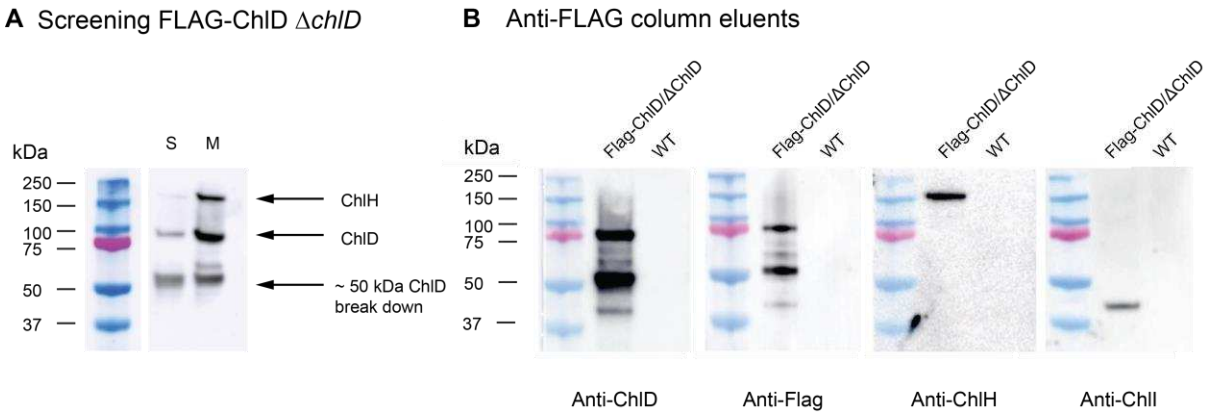

Figure 1: Purification of FLAG-ChlD-ChlH-ChlI complex from *Synechocystis* cells.
(A) FLAG-ChlD Δ*chlD Synechocystis* soluble and detergent solubilised extracts were applied to an anti-FLAG column to optimise purification conditions. Proteins were separated by 12 % Bis-Tris SDS-PAGE, electro-transferred to a PVDF membrane and probed with antibodies for ChlH and ChlD. Lanes: S, soluble fraction elution; M, membrane fraction elution. The ChlD-ChlH complex detected in both soluble and membrane fractions, with larger amounts of both proteins present in the membrane fraction. **(B)** Probing with antibodies for each

chelatase subunit in FLAG-ChlD Δ*chlD Synechocystis* and wild type (WT) *Synechocystis* membrane fractions eluted from a FLAG column revealed that the three constituent proteins of MgCH can all be co-purified from solubilised membranes when there is a N-terminal FLAG tag on ChlD.

A ChlH-ChlD complex can be copurified when the subunits are recombinantly produced in *E. coli*.

Genes encoding a N-terminal StrepII-tagged ChlH and untagged ChlD from *Synechocystis* were co-expressed in *E. coli*. Proteins were purified by StrepTactin affinity chromatography, using low salt buffers to retain subunit interactions. Analysis by SDS-PAGE showed bands at 150 kDa and 75 kDa corresponding to the molecular masses of ChlH and ChlD respectively (Fig. 2 A).Western blot analysis of the supernatant and major elution fraction (E2) confirmed that ChlD copurified with tagged ChlH (Fig. 2B). A control experiment where only non-tagged ChlD was applied to the StrepTactin Sepharose did not show any significant quantity of ChlD binding to or eluting from the column (Fig. S2).

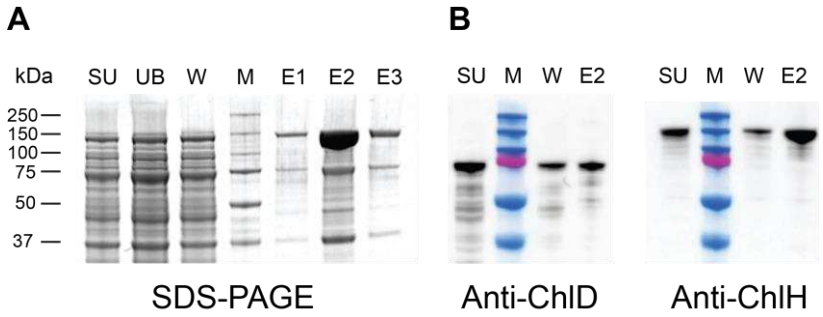

Figure 2: Copurifying recombinant ChlD and ChlH

(A) *Synechocystis* StrepII-ChlH was co-produced with non-tagged ChlD and purified on a StrepTrap HP column. Lanes: SU, cell supernatant; UB, unbound fraction; M, molecular weight markers as indicated on right hand side; W, Binding buffer wash, Elutions (E1 – 3): Binding buffer with 2.5 mM biotin. **(B)** Western blot analysis of StrepII-ChlH and non-tagged ChlD fractions from **A**, showing the presence of ChlD in both the supernatant and elution fraction.

Quantitative analysis of binding between ChlD and ChlH.

Purified recombinant ChlH and ChlD proteins from *Synechocystis* were produced separately in *E. coli,* then MST was used to determine the binding affinity of ChlD to ChlH in the

absence of other subunits or any substrates [11]. ChlD was titrated into a constant concentration of labelled ChlH. Dissociation constants (K_d) values were calculated using a single-site binding model using the MO.Affinity Software (Nanotemper) supplied with the instrument. The interaction between ChlH and ChlD proved to be Mg^{2+} dependent, and a K_d of 331 ± 58 nM was obtained in the presence of 10 mM Mg^{2+}, and increased by an order of magnitude to 2089 ± 387 nM in the absence of Mg^{2+} (Fig. 3, Table 1). Control experiments to determine the assembly state of both ChlH and ChlD within the binding titrations (Sup Fig. S3) indicate that labelled ChlH is a monomer at the 20 nM concentration in the assay, and that assembly into higher order species only occurs at concentrations higher than 100 nM. ChlD self-assembles to form a dimer under these experimental conditions, with a calculated K_d of 296 nM. There is no indication from the ChlD-ChlD titration that any higher order multimers are being formed within the concentration range of the binding studies presented in this work. This would indicate that the ChlD-ChlH titrations initially represent a monomer of ChlD interacting with ChlH, after which the dimer form of ChlD will likely form the majority of interactions with a monomer of ChlH. Only slight deviations from a single site binding curve are seen in these data suggesting that more complex assembly modelling is not worthwhile in this case. We emphasise that the measured K_d values for the ChlH-ChlD and ChlH-ChlD mutant interactions may include components of the ChlD dimerization and this value should be treated as an empirical description of the interaction between ChlH and all oligomeric states of ChlD.

Table 1:Dissociation constant (K_d) values for the ChlD-ChlH interaction of the ChlD mutants.

ChlD mutant	Mutation type	Mg^{2+} present K_d / µM	Mg^{2+} free K_d / µM
Wild type		0.331 ± 0.058	2.10 ± 0.387
Truncation A	N-terminal truncation[(1)] AAA^+ domain alone	14.6 ± 2.99	5.93 ± 1.08
Truncation B	N-terminal truncation[(1)] AAA^+ and PP domain	10.5 ± 1.9	6.76 ± 1.52
QuinE	Allosteric response to	0.339 ± 0.040	0.512 ± 0.161

	Mg^{2+} (2)		
D487E	MIDAS motif	0.842 ± 0.162	1.489 ± 0.221
S489A	MIDAS motif	1.98 ± 0.52	3.21 ± 0.76
S491A	MIDAS motif	0.147 ± 0.026	0.351 ± 0.097
S554R	MIDAS motif	0.481 ± 0.140	0.988 ± 0.126

K_d reported to 3 significant figures, errors reported as ± the estimated standard deviation of the K_d. Each K_d is determined from 3 independent biological repeats, errors reported are from non-linear regression. Constructs originally described in (1) Adams *et al.* [11] and (2) Brindley *et al.* [13].

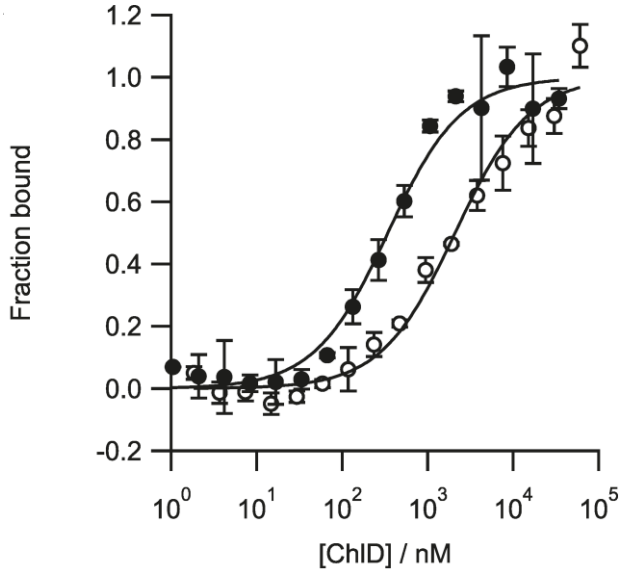

Figure 3: Quantifying the assembly of the ChlD-ChlH complex. (A) The presence of magnesium increases the strength of the ChlD-ChlH interaction. Thermophoresis was performed where ChlD was titrated into 20 nM labeled ChlH with or without 10 mM Mg^{2+} in 50 mM Tris/NaOH, 0.2% Pluronic-F127, pH 7.8. The interaction shows a higher affinity at 10 mM Mg^{2+} (filled circles) compared with Mg^{2+} free (open circles). Each data point represents the average of three independent biological repeats, with the standard deviation represented by error bars. Fitting of the resultant binding isotherms revealed K_d values of 331.99 ± 58 nM and 2088.9 ± 387 nM for Mg^{2+} present and Mg^{2+} free, respectively.

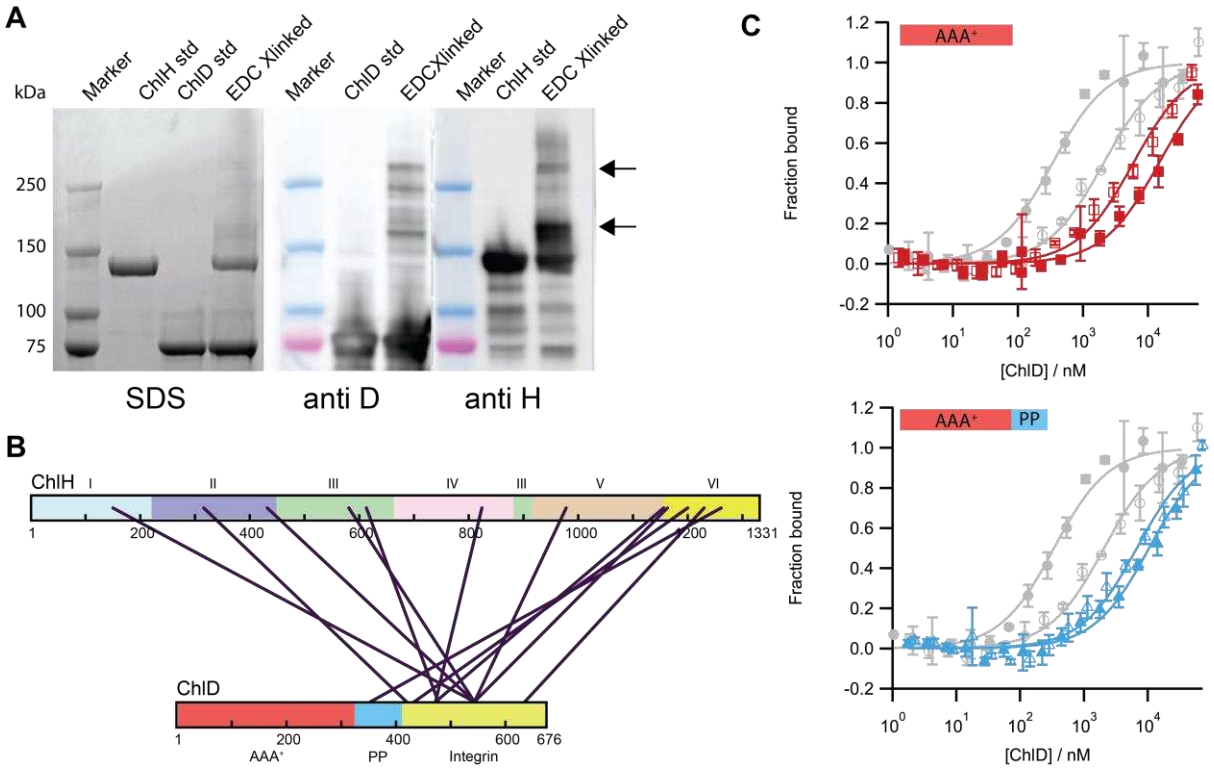

Figure 4: Capturing the ChlD-ChlH complex. (A) SDS-PAGE analysis of chemically crosslinked proteins. 1 mg ml^{-1} ChlH was crosslinked with 1 mg ml^{-1} ChlD using EDC (see methods); immunoblotting shows high molecular weight bands containing both ChlH and ChlD (indicated by arrows). Lanes as labelled above. (B) Bands indicated by arrows in (A) were subjected to in-gel digestion with trypsin and analysed for EDC-crosslinked residues by mass spectrometry; the primary sequence of the ChlH and ChlD proteins are presented as rectangles with residue numbers marked. For ChlH, the six domains are numbered as in Chen *et al* [18]. The AAA^+ (red), acidic poly proline region (PP) (blue) and the C-terminal Integrin domain (yellow) domains of ChlD are indicated. Purple lines denote chemical crosslinks between ChlH and ChlD. (C) MST assays to measure binding of C-terminal truncations of ChlD to ChlH. Truncations consisted of either the AAA^+ domain alone (red isotherm), or the AAA^+ domain with the polyproline region (blue isotherm). Closed markers, 10 mM free Mg^{2+}; open markers, no free Mg^{2+}. For comparison WT ChlD isotherms are shown in grey.

Subunit interactions within the ChlH-ChlD complex

Chemical crosslinking was employed to gain an insight into the physical location of the interaction site between ChlH and ChlD. The water-soluble zero length 1-ethyl-3-(3-dimethylaminopropyl)carbodimide hydrochloride (EDC) crosslinker was used, which produced higher molecular weight bands (highlighted with arrows in Fig. 4A) in

SDS-PAGE and immunoblot analyses. The bands denoted by arrows in Fig. 4A were excised from the gel, and subjected to in-gel tryptic digestion. Mass spectrometry analysis of the resultant peptides showed that the majority of crosslinks appear to occur between the C-terminal integrin I domain of ChlD (shown in yellow in Fig. 4B) and the 'body' region of ChlH (domains III – VI), although there is also a crosslink in the head region (domain I) of ChlH from residues 150 - 173 (Fig. 4 B, Table S4 and S5).

C-terminal truncations of ChlD dramatically weaken the interaction with ChlH

We have previously shown that the N-terminal AAA^+ domain of ChlD is primarily responsible for the interaction that forms the ChlID motor complex [11]. Cross-linking of ChlH to ChlD (Fig. 4B) shows that the majority of interactions with ChlH involve the C-terminal domain of ChlD, but a cross-link with the PP region suggested the N-terminal domain ChlD may also be in close proximity to ChlH. As a test, we used MST to measure the extent to which C-terminal truncations of ChlD retain the capacity to bind to ChlH. These truncation mutants consisted of either the AAA^+ domain alone (truncation A, Fig. 4C, red isotherm), or the AAA^+ domain with the polyproline region (truncation B, Fig. 4C, blue isotherm). The C-terminal truncation mutants show an almost 50-fold higher K_d compared to wild-type, which weakens even further in the presence of Mg^{2+}; this is in stark contrast to the wild-type which shows an order of magnitude tighter binding in the presence of Mg^{2+} (Table 1). Thus, mass spectrometry and MST show that the C-terminal integrin I domain of ChlD is the major determinant of binding to ChlH. In the Luo *et al* study [15], where recombinant proteins from rice are used, their results suggest that only the AAA^+ and linker domains are required for protein activity, results that directly contradict this work, previous studies from our laboratory [11, 13] and that of other groups [14]. While it is possible that higher plant enzymes have evolved different interaction sites between the ChlD and ChlH proteins, the proposals of Luo *et al.* [15] require biophysical characterization of the protein-protein interactions of the rice proteins.

The ChlH-ChlD interaction mediates the cooperative response of the *Synechocystis* chelatase to magnesium

The chemical cross-linking and truncation binding studies indicated that the integrin I domain is the primary driver of the interaction between ChlH and ChlD. Previously we showed that five glutamate residues in the C-terminal region of ChlD (E510, E513, E600, E603 and E605) regulate the cooperative response to Mg^{2+} observed in chelatase assays in the *Synechocystis*

enzyme [13]. Binding studies were performed between ChlH and a quintuplet mutant of ChlD with these five glutamate residues altered, to see if the Mg^{2+} dependent decrease in K_d for the ChlH-ChlD association observed in Fig. 3A was related to this cooperativity. The five glutamate residues are replaced with the corresponding residues found in the non-cooperative *T. elongatus* ChlD subunit (E510Q/E513Q/E600T/E603P/E605T). In the presence of Mg^{2+} this mutant (ChlD QuinE) has a K_d for ChlH similar to the wild-type protein, which is essentially unchanged in the absence of Mg^{2+}. This results suggests that Mg^{2+} dependent regulation of the ChlH-ChlD interaction is the source of this cooperativity (Fig. S4).

The metal ion dependent adhesion site (MIDAS) is essential for MgCH catalysis

Integrin I domains are are often involved in Mg^{2+} dependent protein-protein interactions, mediated by a MIDAS motif (DXSXS where X is any residue) that coordinates a Mg^{2+} ion; completion of the magnesium coordination sphere with a ligand from the second protein is presumed to stabilize the protein-protein interaction [38]. Previous studies on the MgCH BchD subunit from from bacteriochlorophyll-syntheising *Rhodobacter capsulatus* [14] also provide evidence of the importance of this region in either protein-protein interactions or catalysis.

A homology model for this integrin I domain of ChlD was produced to aid investigation of the MIDAS region. 21 % sequence identity was found between residues 481-672 of the *Synechocystis* enzyme and the extracellular domain of human Tumor Endothelial Marker 8 (TEM8, PDB accession code: 3N2N) [39]. The resulting alignment was used with Modeller [37] to generate multiple homology models, with the best one chosen by Modeller's inbuilt DOPE score [40].

With the aid of the homology model (Fig. 5A), a series of point mutations was created to probe the MIDAS motif. Type I mutants (D487E, S489A and S491A; we could only produce low levels of the D487A mutant) perturbed metal binding. The serine mutants lose a putative ligand for Mg^{2+} while the aspartate to glutamate mutation was predicted to add a steric clash with the Mg^{2+}. The type II mutant (S554R) introduced an Arg residue, blocking metal binding whilst providing a replacement positive charge. All the recombinant proteins purified as wild type (apart from D487A); their CD spectra were consistent with folded protein, and their melting temperatures were above the standard chelatase assay temperature of 34 °C (Fig. S5 and S6, Table S6).

All the variant proteins were inactive, except for S554R which has relative rate of *ca.* 5 % of that of the wild type protein (Fig. S7). To investigate whether the lack of activity was due to a decreased affinity for ChlH, MST was performed on each of the MIDAS mutants in the presence or absence of Mg^{2+} (Fig. 5B - F). The K_d values (Table 1) show that all mutants are able to bind ChlH at least as well as the WT in the absence of Mg^{2+}, with ChlD S491A appearing to have a greater affinity for ChlH than WT, especially in Mg^{2+} free conditions. The only active mutant, S554R, has a K_d value for ChlH roughly similar to that of WT protein. While integrin I domains are generally involved in cell-protein interactions in the case of the S554R mutant, which mimics the charge of a ligated Mg^{2+} ion, the correct ChlD-H association may occur to allow power to be transferred from the ChlID complex. However the lowered chelatase rate implies that the the ChlD-ChlH interaction can still occur if the positive charge associated with the chelated Mg^{2+} in the MIDAS motif is replaced by a positively charged amino acid, although a correctly ligated Mg^{2+} ion in the MIDAS domain is undoubtably important for full chelatase activity.

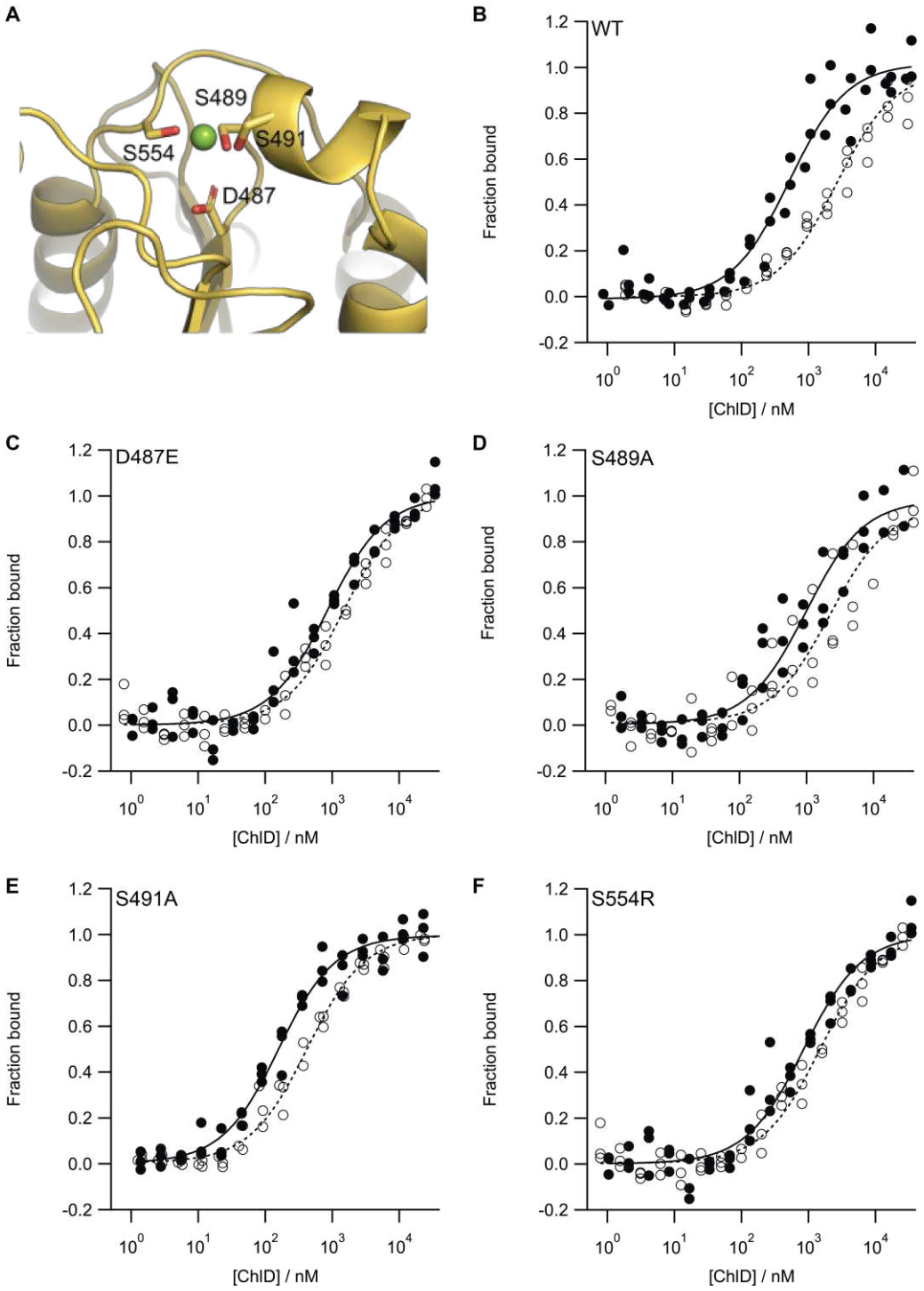

Figure 5: MIDAS mutants of ChlD continue to form a ChlD-ChlH complex. (A) Model structure of the MIDAS motif of ChlD and MST binding isotherms of (B) WT and (C-F) MIDAS mutants. In the model structure, ChlD is represented as a cartoon with predicted Mg^{2+} binding residues represented as sticks. MST assays were performed in the presence (closed circles) and absence (open circles) of 10 mM Mg^{2+}. MST experiments were performed in triplicate from independent batches of protein. K_d values are shown in Table 1.

Conclusion

Magnesium chelatase is responsible for the initiation of one of the most important biochemical pathways on Earth, the biosynthesis of (bacterio)chlorophyll. Understanding how this pivotal enzyme transfers the free energy gained from the hydrolysis of $MgATP^{2-}$ at the AAA^+ motor to the active site where chelation takes place is vital, not only for revealing the mechanism of MgCH, but also in our broader understanding of allosteric circuits within the AAA^+ superfamily of motors. While much work has taken place to understand the individual roles of the subunits within MgCH, only now are we starting to understand the protein-protein interactions that are involved in forming the catalytic ChlIDH complex. Identification of protein-protein interaction domains and motifs will facilitate the elucidation of the stoichometry of the subunits within the active complex, the allosteric circuits which regulate movement of chemomechanical motion through the complex, and ultimately the structure and mechanism of the enzyme.

In this study we combined *in vivo* and *in vitro* analyses of the *Synechocystis* MgCH complex. Through a combination of co-purification of native and recombinant MgCH, XL-MS and thermophoretic analysis we show that the ChlID AAA^+ motor interacts with the the ChlH chelation subunit via a link between ChlH and ChlD. This is primarily through the C-terminal integrin I domain of ChlD; mutagenesis of key residues in the integrin I domain MIDAS motif established its importance for forming the active chelatase enzyme.

While it is known that ChlD and ChlI form a complex [8,12], the connection between ChlID and ChlH was less well defined. Previous studies have described the importance of the polyproline linker and AAA^+ domain in ChlD to the activity of MgCH [12,15,41,42], but there has been limited description of the role of the C-terminal integrin I domain of ChlD, other than the work of Axelsson *et al.* which revealed the importance of the MIDAS residues for chelatase activity [14]. Our work has provided a biochemical and kinetic counterpart to the results of the recent study by Luo *et al.* [15], which used yeast two-hybrid analysis to show that ChlD interacts with ChlH, although our work proposes a different location for this protein-protein interaction. We have previously shown that C- and N-terminal truncations of ChlD from *Synechocystis* and *Thermosynechoccus elongatus* are not able to produce active chelatases [11,13], and that the N-terminal AAA^+ domain of ChlD is primarily responsible for interaction with ChlI [11].

FUNDING INFORMATION

A.A.B., A.H., C.N.H, J.D.R., and N.B.P.A. gratefully acknowledge financial support from the Biotechnology and Biological Sciences Research Council (BBSRC U.K.), award number BB/M000265/1. C.N.H., P.J.J. and A.A.B were also supported by Advanced Award 338895 from the European Research Council. M.J.D. was supported by BBSRC U.K. award number BB/M012166/1. D.F. was supported by a University of Sheffield doctoral scholarships.

DECLARATIONS OF INTEREST

The authors declare that they have no conflicts of interest with the contents of this article.

AUTHOR CONTRIBUTIONS

A.A.B, C.N.H, J.D.R and N.B.P.A designed the experiments. D.F., A.A.B., A.H., P.J.J., B.J., N.B.P.A. performed the experiments. M.J.D. analysed data and provied laboratory space for mass spectrometry experiments. D.F., C.N.H., J.D.R. and N.B.P.A. wrote the manuscript. All authors proof read and approved the manuscript.

References

1 Gibson, L. C., Willows, R. D., Kannangara, C. G., von Wettstein, D. and Hunter, C. N. (1995) Magnesium-protoporphyrin chelatase of Rhodobacter sphaeroides: reconstitution of activity by combining the products of the bchH, -I, and -D genes expressed in Escherichia coli. Proc. Natl. Acad. Sci. U. S. A. **92**, 1941–1944.

2 Jensen, P. E., Gibson, L. C., Henningsen, K. W. and Hunter, C. N. (1996) Expression of the chlI, chlD, and chlH genes from the Cyanobacterium synechocystis PCC6803 in Escherichia coli and demonstration that the three cognate proteins are required for magnesium-protoporphyrin chelatase activity. J. Biol. Chem. **271**, 16662–16667.

3 Willows, R. D. (1996) Three separate proteins constitute the magnesium chelatase of Rhodobacter sphaeroides. Eur. J. Biochem. **235**, 438–443.

4 Adams, N. B. P., Brindley, A. A., Hunter, C. N. and Reid, J. D. (2016) The catalytic power of magnesium chelatase: a benchmark for the AAA^{+}ATPases. FEBS Lett.**590**, 1687-1693.

5 Reid, J. D. and Hunter, C. N. (2004) Magnesium-dependent ATPase activity and cooperativity of magnesium chelatase from Synechocystis sp. PCC6803. J. Biol. Chem. **279**, 26893-26899.

6 Hanson, P. I. and Whiteheart, S. W. (2005) AAA+ proteins: have engine, will work. Nat. Rev. Mol. Cell Biol. **6**, 519–529.

7 Reid, J. D., Siebert, C. A., Bullough, P. A. and Hunter, C. N. (2003) The ATPase activity of the ChlI subunit of magnesium chelatase and formation of a heptameric AAA+ ring. Biochemistry **42**, 6912–6920.

8 Jensen, P. E., Gibson, L. and Hunter, C. N. (1999) ATPase activity associated with the magnesium-protoporphyrin IX chelatase enzyme of Synechocystis PCC6803: evidence for ATP hydrolysis during Mg2+ insertion, and the MgATP-dependent interaction of the ChlI and ChlD subunits. Biochem. J. **339**, 127-134.

9 Fodje, M. N., Hansson, A., Hansson, M., Olsen, J. G., Gough, S., Willows, R. D. and Al-Karadaghi, S. (2001) Interplay between an AAA module and an integrin I domain may regulate the function of magnesium chelatase. J. Mol. Biol. **311**, 111–122.

10 Adams, N. B. P. and Reid, J. D. J. D. (2012) Nonequilibrium isotope exchange reveals a catalytically significant enzyme-phosphate complex in the ATP hydrolysis pathway of the AAA+ ATPase magnesium chelatase. Biochemistry **51**, 2029–2031.

11 Adams, N. B. P., Vasilev, C., Brindley, A. A. and Hunter, C. N. (2016)

Nanomechanical and Thermophoretic Analyses of the Nucleotide-Dependent Interactions between the AAA + Subunits of Magnesium Chelatase. J. Am. Chem. Soc. **138**, 6591–6597.

12 Adams, N. B. P. and Reid, J. D. (2013) The Allosteric Role of the AAA + Domain of ChlD Protein from the Magnesium Chelatase of Synechocystis Species PCC 6803. J. Biol. Chem. **288**, 28727–28732.

13 Brindley, A. A., Adams, N. B. P., Hunter, C. N. and Reid, J. D. (2015) Five Glutamic Acid Residues in the C-Terminal Domain of the ChlD Subunit Play a Major Role in Conferring Mg 2+ Cooperativity upon Magnesium Chelatase. Biochemistry **54**, 6659–6662.

14 Axelsson, E., Lundqvist, J., Sawicki, A., Nilsson, S., Schröder, I., Al-Karadaghi, S., Willows, R. D. and Hansson, M. (2006) Recessiveness and dominance in barley mutants deficient in Mg-chelatase subunit D, an AAA protein involved in chlorophyll biosynthesis. Plant Cell **18**, 3606–3616.

15 Luo, S., Luo, T., Liu, Y., Li, Z., Fan, S. and Wu, C. (2018) N-terminus plus linker domain of Mg-chelatase D subunit is essential for Mg-chelatase activity in Oryza sativa. Biochem. Biophys. Res. Commun. **497**, 749-755.

16 Karger, G. A., Reid, J. D. and Hunter, C. N. (2001) Characterization of the binding of deuteroporphyrin IX to the magnesium chelatase H subunit and spectroscopic properties of the complex. Biochemistry **40**, 9291–9299.

17 Sirijovski, N., Lundqvist, J., Rosenbäck, M., Elmlund, H., Al-Karadaghi, S., Willows, R. D. and Hansson, M. (2008) Substrate-binding model of the chlorophyll biosynthetic magnesium chelatase BchH subunit. J. Biol. Chem. **283**, 11652–11660.

18 Chen, X., Pu, H., Fang, Y., Wang, X., Zhao, S., Lin, Y., Zhang, M., Dai, H.-E., Gong, W. and Liu, L. (2015) Crystal structure of the catalytic subunit of magnesium chelatase. Nat. Plants, **1**, 15125.

19 Gibson, L., Jensen, P. E. and Hunter, C. N. (1999) Magnesium chelatase from Rhodobacter sphaeroides: initial characterization of the enzyme using purified subunits and evidence for a BchI-BchD complex. Biochem. J. **337**, 243-251.

20 Hynes, R. O. (2002) Integrins : Bidirectional , Allosteric Signaling Machines. Cell. **110**, 673–687.

21 Lake, V., Olsson, U., Willows, R. D. and Hansson, M. (2004) ATPase activity of magnesium chelatase subunit I is required to maintain subunit D in vivo. Eur. J. Biochem. **271**, 2182–2188.

22 Davison, P. A., Schubert, H. L., Reid, J. D., Iorg, C. D., Heroux, A., Hill, C. P. and Hunter, C. N. (2005) Structural and Biochemical Characterization of Gun4 Suggests a Mechanism for Its Role in Chlorophyll Biosynthesis. Biochemistry **44**, 7603–7612.

23 Walker, C. J. and Weinstein, J. D. (1994) The magnesium-insertion step of chlorophyll biosynthesis is a two-stage reaction. Biochem. J. **299**, 277–284.

24 Walker, C. J. and Weinstein, J. D. (1991) Further characterization of the magnesium chelatase in isolated developing cucumber chloroplasts : substrate specificity, regulation, intactness, and ATP requirements. Plant Physiol. **95**, 1189–1196.

25 Adams, N. B. P., Marklew, C. J., Brindley, A. A., Hunter, C. N. and Reid, J. D. (2014) Characterization of the magnesium chelatase from Thermosynechococcus elongatus. Biochem. J. **457**, 163–170.

26 Jensen, P. E., Gibson, L. C. and Hunter, C. N. (1998) Determinants of catalytic activity with the use of purified I, D and H subunits of the magnesium protoporphyrin IX chelatase from Synechocystis PCC6803. Biochem. J. **334,** 335–344.

27 Viney, J., Davison, P. A., Hunter, C. N. and Reid, J. D. (2007) Direct measurement of metal-ion chelation in the active site of the AAA+ ATPase magnesium chelatase. Biochemistry **46**, 12788–12794.

28 Rippka, R., Deruelles, J., Waterbury, J. B., Herdman, M., Stanier, R. Y., Deruelles, J., Rippka, R., Herdman, M. and Waterbury, J. B. (1979) Generic Assignments, Strain Histories and Properties of Pure Cultures of Cyanobacteria. Microbiology **111**, 1–61.

29 Hollingshead, S., Kopecná, J., Jackson, P. J., Canniffe, D. P., Davison, P. A., Dickman, M. J., Sobotka, R. and Hunter, C. N. (2012) Conserved chloroplast open-reading frame ycf54 is required for activity of the magnesium protoporphyrin monomethylester oxidative cyclase in Synechocystis PCC 6803. J. Biol. Chem., **287**, 27823–27833.

30 Cereda, A., Hitchcock, A., Symes, M. D. M. D., Cronin, L., Bibby, T. S. T. S. and Jones, A. K. A. K. (2014) A bioelectrochemical approach to characterize extracellular electron transfer by synechocystis sp. PCC6803. PLoS One **9**, e91484.

31 McGoldrick, H. M., Roessner, C. A., Raux, E., Lawrence, A. D., McLean, K. J., Munro, A. W., Santabarbara, S., Rigby, S. E. J., Heathcote, P., Scott, A. I., et al. (2005) Identification and Characterization of a Novel Vitamin B 12 (Cobalamin) Biosynthetic Enzyme (CobZ) from Rhodobacter capsulatus , Containing Flavin, Heme, and Fe-S Cofactors. J. Biol. Chem. **280**, 1086–1094.

32 Ritchie, R. J. (2006) Consistent sets of spectrophotometric chlorophyll equations for

acetone, methanol and ethanol solvents. Photosynth. Res. **89**, 27-41.

33 Pandey, A., Andersen, J. S. and Mann, M. (2000) Use of Mass Spectrometry to Study Signaling Pathways. Sci. Signal. **2000**, l1–l1.

34 Hollingshead, S., Kopečná, J., Armstrong, D. R., Bučinská, L., Jackson, P. J., Chen, G. E., Dickman, M. J., Williamson, M. P., Sobotka, R. and Hunter, C. N. (2016) Synthesis of Chlorophyll-Binding Proteins in a Fully Segregated Δycf54 Strain of the Cyanobacterium Synechocystis PCC 6803. Front. Plant Sci. **7**, 292.

35 Sigrist, C. J., Cerutti, L., Hulo, N., Gattiker, A., Falquet, L., Pagni, M., Bairoch, A. and Bucher, P. (2002) PROSITE: a documented database using patterns and profiles as motif descriptors (available at http://www.expasy.ch/prosite). Br. Bioinforma. **3**, 265–274.

36 Zimmermann, L., Stephens, A., Nam, S. Z., Rau, D., Kübler, J., Lozajic, M., Gabler, F., Söding, J., Lupas, A. N. and Alva, V. (2017) A Completely Reimplemented MPI Bioinformatics Toolkit with a New HHpred Server at its Core. J. Mol. Biol. **430**, 2237-2243.

37 Webb, B. and Sali, A. (2014) Comparative Protein Structure Modeling Using MODELLER. In Current Protocols in Bioinformatics, pp 5.6.1-5.6.32, John Wiley & Sons, Inc., Hoboken, NJ, USA.

38 Luo, B., Carman, C. V. and Springer, T. A. (2007) Structural Basis of Integrin Regulation and Signaling. Annu. Rev. Immunol. **25**, 619–647.

39 Fu, S., Tong, X., Cai, C., Zhao, Y., Wu, Y., Li, Y., Xu, J., Zhang, X. C., Xu, L., Chen, W., et al. (2010) The structure of tumor endothelial marker 8 (TEM8) extracellular domain and implications for its receptor function for recognizing anthrax toxin. PLoS One **5**, e11203.

40 Shen, M. and Sali, A. (2006) Statistical potential for assessment and prediction of protein structures. Protein Sci. **15**, 2507–2524.

41 Papenbrock, J., Gräfe, S., Kruse, E., Hänel, F. and Grimm, B. (1997) Mg-chelatase of tobacco: identification of a Chl D cDNA sequence encoding a third subunit, analysis of the interaction of the three subunits with the yeast two-hybrid system, and reconstitution of the enzyme activity by co-expression of recombinant CHL D, CHL H and CHL I. Plant J. **12**, 981–990.

42 Grafe, S., Saluz, H.-P., Grimm, B. and Hanel, F. (1999) Mg-chelatase of tobacco: The role of the subunit CHL D in the chelation step of protoporphyrin IX. Proc. Natl. Acad. Sci. **96**, 1941–1946.

Strain	Description	Source
WT	Glucose tolerant wild-type strain of *Synechocystis* sp. PCC 6803.	Dr Roman Sobotka, Centre Algatech, Czech Republic
FLAG-ChlD	Gene encoding 3×FLAG tagged ChlD expressed from *psbAII* promoter. Kanamycin resistant.	This study
FLAG-ChlD Δ*chlD*	Native *chlD* (slr1777) deleted from FLAG-ChlD strain. Kanamycin and zeocin resistant.	This study

S1 Table. Strains of *Synechocystis* used in this study

Primer name	Sequence (5´to 3´)
AH47	AAACGCCCTCTGTTTACCCA
AH48	TCAACCCGGTACAGAGCTTC
AH282	ATTTGGCGGCCGCAACCACCCTGACCCCCTTTATTC
AH283	ACTAAAGATCTCTATTGCATGTCGGCGATCGCCTGG
AH434	TCAATGGCATCCAGTTTGAC
AH435	ACATTAATTGCGTTGCGCTCACTGCGGAAATTGAGGGGAATAAAGG
AH436	CAACTTAATCGCCTTGCAGCACATGACCAAGGTATTGCCTCCATG
AH437	AGACCAGTCTGAGGCTCTAGTCC
AH438	CTGGGTTTCCAATTGATCCAGG

S2 Table. Primers used for generating *Synechocystis* FLAG-ChlD *ΔchlD strains* used in this study.

ChlD variant	Forward Primer (5´to 3´)	Reverse Primer (5´to 3´)
D487E	TTGTGTTTTTGGTGGAAGCGTCGGGTTCCATGG	ATGGAACCCGACGCTTCCACCAAAAACAC
S489A	TTGGTGGATGCGGCGGGTTCCATGG	AACGCCATGGAACCCGCCGCATCCACC
S491A	ATGCGTCGGGTGCCATGGCGTTGAATCG	ATTCAACGCCATGGCACCCGACGCATCC
S554R	TTGCCCTGTGGCGGTGGTCGTCCCCTTTCC	AAGCCGTGGGAAAGGGGACGACCACCGCCACAGG

S3 Table. Primers used for generating MIDAS site directed mutants of ChlD used in this study.

Gel band	Protein	-(log_{10} p-value)	No. of peptide spectrum matches	Sequence coverage (%)
Upper (*ca.* 470 kDa*)*	ChlH	657	547	50.6
	ChlD	456	421	57.4
Lower (*ca.* 370 kDa)	ChlH	1980	1239	80.8
	ChlD	929	745	79.7

S4 Table. Analysis by mass spectrometry of native-PAGE gel bands corresponding to putative ChlH-ChlD complexes. Bands were excised and the proteins subjected to in-gel digestion with trypsin. Peptides were extracted and analysed by nanoLC-MS/MS. Protein components were identified by database searching as described in Experimental Procedures. The p-value is the probability that the protein identification is due to random events.

Peptide in ChlH	Crosslinked site in ChlH	Peptide in ChlD	Crosslinked site in ChlD	No. of peptide spectrum matches	Best 2-D PEP
K.**E**NSSGAGFQDAMLK.L	E150	K.**K**R.L	K543	5	3.2E-7
R.L**E**AIAQR.A	E432	K.**K**R.L	K543	1	1.3E-3
K.EFGNVFIGVQPTFGY**E**GDPMR.L	E581	K.**K**R.L	K543	1	1.8E-9
R.SASPHHGFAAYYTYLNHIWKA**D**AVLHFGT HGSLEFMPGK.Q	D613	K.LVR**K**AGALIVFLVDASGSMALNR.M	K477	1	2.7E-3
R.NSDKGILA**D**VELLQDITLATR.A	D824	R.QVIVEQGDIRG**K**K.L	K472	1	5.3E-7
R.AENGGNYP**E**TIASVLWGTDNIK.T	E978	K.**K**R.L	K543	1	7.4E-4
K.TA**D**ATFQNLDSSEISLTDVSHYFDSDPTK.L	D1156	R.G**K**K.L	K472	1	1.6E-9
K.TADATFQNL**D**SSEISLTDVSHYFDSDPTK.L	D1163	K.**K**R.L	K543	1	1.0E-12
K.APAAYIA**D**TTTANAQVR.T	D1200	K.G**K**.V	K433	4	2.0E-8
K.WY**E**GMLSHGYEGVR.E	E1230	K.**K**FVSTGFGK.E	K635	2	2.7E-7
R.LVNTMGWSATAGAV**D**NWVYEDANSTFIK .D	D1261	R.QAVELVIVPRSVLMDNPPPPEQAPPPPPPP QNQDEG**K**DEQEDQQDDK.E	K353	1	4.0E-6

S5 Table. XL-MS of a putative ChlH-ChlD complex using 1-ethyl-3-(3-dimethylamnopropyl)carbodiimide-HCl (EDC). These results were generated as in S2 Table. Crosslinked residues are highlighted in bold within the peptide sequences. 2-Dimensional posterior error probability (2-D PEP) is the probability that a peptide spectrum match is a random event.

ChlD MIDAS Mutant	T_m / °C
WT	50
D487E	47
S489A	60
S491A	46
S554R	54

S6 Table. Melting temperatures of ChlD MIDAS Mutants. The thermal stabilities of all of the mutants are comparable to WT and well above the 34 °C used in assays. This would suggest that instability of the mutants is not the cause of the abolished or greatly reduced chelatase activity.

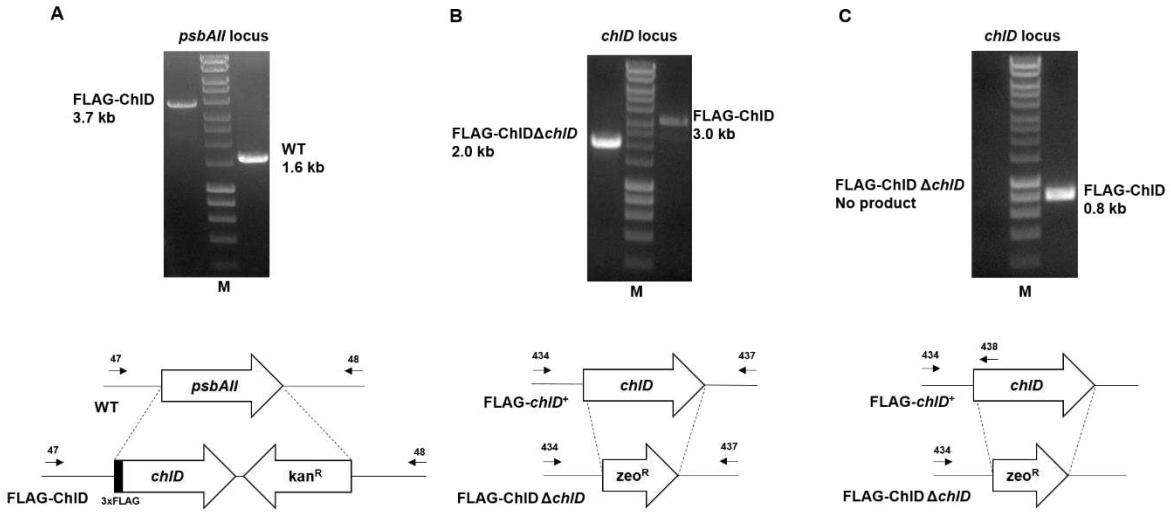

S1 Fig. Generation of *Synechocystis* strains used in this study. A Integration of gene encoding 3×FLAG-tagged ChlD at the *psbAII* (slr1311) locus in strain FLAG-ChlD. Agarose gel analysis with primers flanking the integration site shows that a single larger PCR product is amplified from the FLAG-ChlD genomic (g)DNA compared to that from the wildtype (WT) due to insertion of the tagged gene and the kanamycin resistance cassette (kan^R) in place of *psbII*. **B-C** Deletion of the native *chlD* (slr1777) gene in strain FLAG-ChlD Δ*chlD*. **B** Agarose gel analysis with primers flanking the deletion site shows that a smaller PCR product is amplified from FLAG-ChlD Δ*chlD* gDNA compared to FLAG-ChlD gDNA due to replacement of the *chlD* gene with the smaller zeocin resistance cassette (zeo^R). **C** To confirm that the FLAG-ChlD Δ*chlD* has fully segregated at the *chlD* locus PCR with a reverse primer internal to the deleted portion of the gene was performed. A product is present using FLAG-ChlD gDNA as template but absent when using gDNA from the FLAG-ChlD Δ*chlD* strain. In all panels the position of primers used in the PCR analysis are indicated with small black arrows and lane M contains Hyperladder™ I (Bioline, UK).

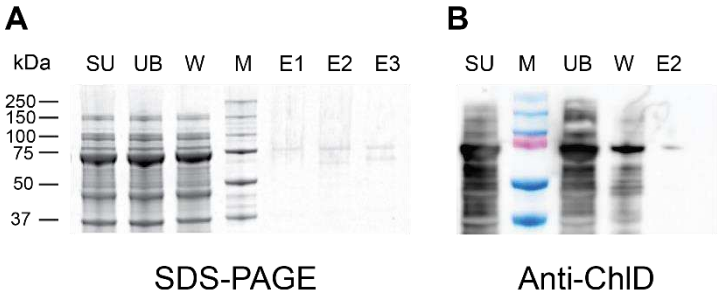

S2 Fig: Non-tagged ChlD does not purify on a StrepTrap column. (A) *Synechocystis* non-tagged ChlD was applied to a StrepTrap HP column. Lanes: SU, cell supernatant; UB, unbound fraction; M, molecular weight markers as indicated on right hand side; W, Binding buffer wash, Elutions (E1 – 3): Binding buffer with 2.5 mM biotin. **(B)** Western blot analysis of StrepII-ChlH and non-tagged ChlD fractions from **A**, showing the presence of ChlD in both the supernatant, unbound and wash fraction, but only a comparitively small amount in the elution fraction.

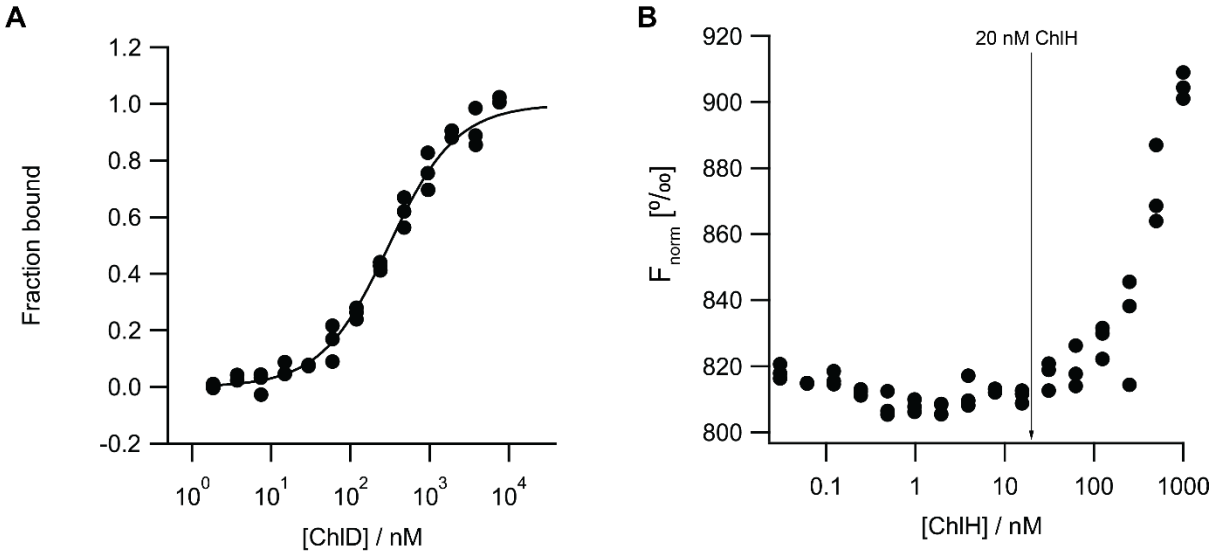

S3 Fig. Monitoring self assembly of (A) ChlD and (B) ChlH. Proteins were labelled with NHS-NT-647 and MST was conducted. (A) A single site binding model fits the data, resulting in a K_d = 296 nM, suggesting that ChlD may be binding to ChlH as a dimer. (B) As indicated by the arrow, there is no observed interaction of ChlH with itself at the concentrations used in ChlD titrations (20 nM). It does seem that ChlH will dimerise at higher concentrations, however. Thermophoresis was performed where each chelatase subunit was titrated into 20 nM labeled of the same subunit in 50 mM Tris/NaOH, 10mM Mg^{2+} 0.2% Pluronic-F127, pH 7.8.

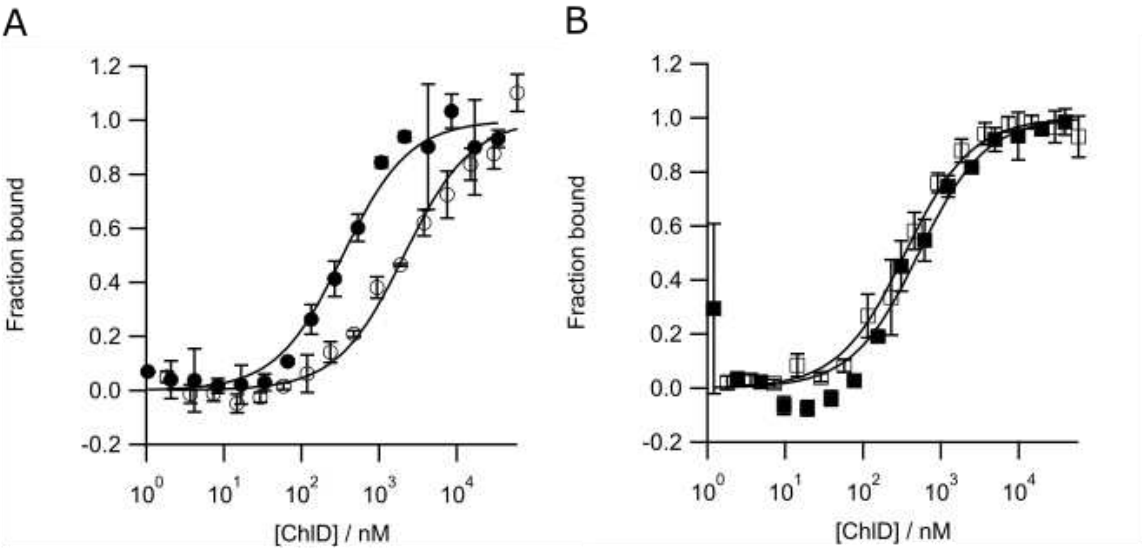

S4 Fig. The Quintuple mutant (QuinE) of ChlD does not have a Mg^{2+} dependent K_d for ChlH. Unlike WT ChlD, the interaction between ChlH and the non-cooperative QuinE mutant of ChlD is not dependent on Mg^{2+}. MST traces of WT (A) and QuinE (B) in the presence and absence of Mg^{2+} (filled and unfilled symbols respectively). The fitted curves reveal a K_d of 338.5 ± 39.7 nM and 512.5 ± 161.31 nM for the QuinE mutant in the presence and absence of Mg^{2+}, respectively.

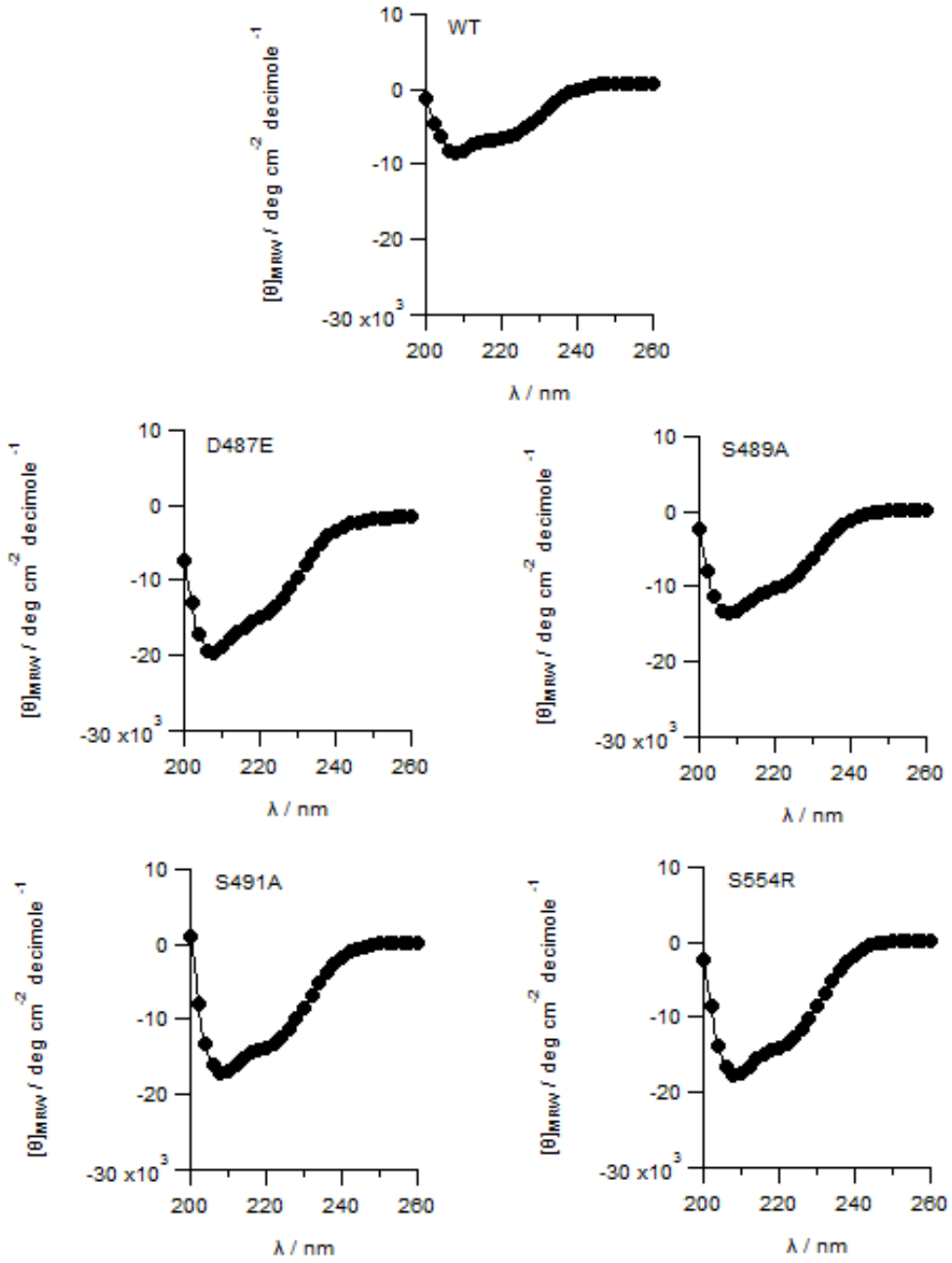

S5 Fig. CD spectra of the ChlD MIDAS mutants. All four mutants have a broadly similar CD spectra to the WT, suggesting that secondary structure of these mutants has not been disrupted. Spectra were recorded with a JASCO-810 spectrometer (JASCO, Great Dunmow, UK). Protein (0.05 mg ml^{-1}) was in a 5 mM sodium phosphate buffer, 1 mM β-mercaptoethanol, pH 7.5. Spectra were recorded from 260 to 200 nm (1 nm steps, 4 s/nm, 4 accumulations) and background subtracted.

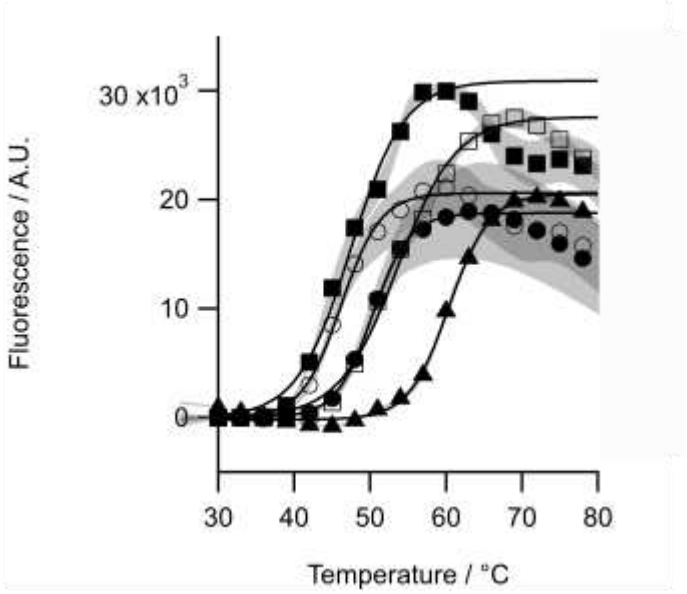

S6 Fig. Temperature stability of MIDAS mutants. All mutants (D487E, filled square; S489A, filled triangle; S491A, open circle; S554R, open square) have a thermal stability comparable or above WT (filled circles), with all calculated T_m values greater than the activity assay temperature of 34 °C. T_m values are shown in Table S4. Assay contained 5 µM ChlD, 10 mM $MgCl_2$, 1x SYPRO Orange and 1x thermal shift buffer. Temperature ramp rate was 1 °C per cycle per minute. Fluorescence was read at each temperature. Every 3 values are shown for clarity, and can be described by equation 3 to calculate T_m values.

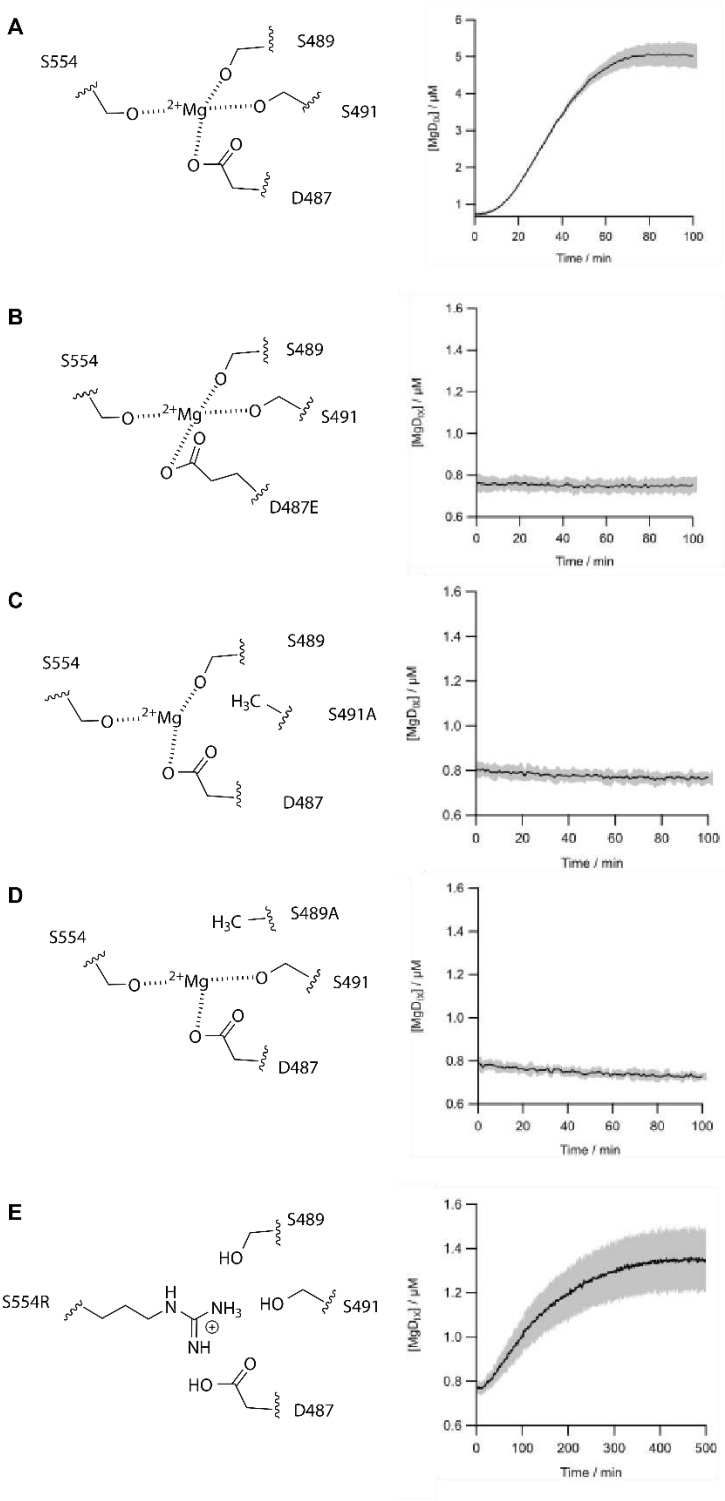

S7 Fig. Activity assays of ChlD MIDAS mutants. Schematic representation of mutant and subsequent chelatase activity of A, WT; B, D487E; C, S491A; D, S489A; and E, S554R. Assays performed under the same conditions as Fig. 3. Of the mutants, only ChlD S554R (open circles) showed any activity, although this was severely impaired when compared to WT (k_{rel} = 5 % c.f. WT ChlD).